



## Seismic Characteristics of the Vulcanian Explosions from the 2003–2005 Eruption at Colima Volcano, Mexico

FRANCISCO JAVIER NÚÑEZ-CORNÚ,<sup>1</sup> JUAN MANUEL ESPÍNDOLA,<sup>2</sup> FIDENCIO ALEJANDRO NAVA PICHARDO,<sup>3</sup> and CARLOS SUÁREZ-PLASCENCIA<sup>1</sup>

**Abstract**—Colima Volcano (19.512°N, 103.617°W, 4000 m.a.s.l.), located on the border between the states of Jalisco and Colima in western Mexico, is the most active volcano in the country. Its activity has taken place through diverse styles of eruption, from very explosive to effusive. In the last decades it has presented frequent vulcanian eruptions with episodes of dome construction–destruction. Four of these cycles occurred from 1990 to 2005, the last one from July 2003 to September 2005. We focus on this last period, for which we analyzed seismic phases and coupled pressure airwaves from high dynamic range seismograms, both in the time and frequency domains, to determine characteristic features, propagation velocities, and origin times for both deep seismic sources and the associated explosions. The results show that the sources of the P-waves associated with the explosions are not located at the summit, but instead at different shallow locations for the different explosions, suggesting the presence of various magmatic pathways within the volcano.

**Key words:** Colima Volcano, Vulcanian explosions, Magmatic pathways, Volcanic seismic signals.

### 1. Introduction

Colima Volcano (19.512°N, 103.617°W, 4000 m.a.s.l.; Fig. 1) is well known for its frequent and varied activity. In the last decades, it has presented several cycles of vulcanian eruptions characterized by dome construction and destruction

(LUHR and CARMICHEL 1990; ROBIN *et al.* 1987). One of these cycles, which occurred in the 1903–1904 period (DÍAZ 1906), preceded the explosive 1913 eruption. More recently Colima has presented four cycles of this type of activity (1991–1994; 1999–2001; 2001–2003; 2004–2005). The characteristics of the first three cycles and, to a certain extent those of the last one, were presented in a preceding paper (NÚÑEZ-CORNÚ *et al.* 2010). In this work, we present the results of our analyses of the vulcanian explosions occurring in 2003 and 2005 corresponding to that cycle. This type of explosive activity is similar to that preceding the 1913 eruption, adding importance to the detailed analysis of the observations of this modern day recurrence.

The general characteristics of the seismicity accompanying this period can be summarized as follows: three explosions occurred during July and August 2003; no further explosions occurred until 2005. In that year, 13 significant explosions occurred from March to September. Contrarily to the behavior observed during previous periods (NÚÑEZ-CORNÚ *et al.* 2010), no relevant precursory activity was detected before the 16 explosions (Fig. 2), suggesting that the volcano is currently in the post brittle/ductile seal-breakage state in the model of FOURNIER (1999). In this work, we focus on the signals associated with these explosions, which have multiple sources such as those arising from the volcanic edifice, from the ground-coupled atmospheric propagation due to the explosion blast, and from the impact of the ejecta.

The complexity of the phenomena taking place during vulcanian eruptions leads to the generation of various types of seismic signals. The waveforms and spectral content of those seismic records are related

<sup>1</sup> Centro de Sismología y Volcanología de Occidente (Sis-Voc), Universidad de Guadalajara, Av. Universidad 203, 48280 Puerto Vallarta, Jal, Mexico. E-mail: pacormu77@gmail.com; carlos.csuarez@gmail.com

<sup>2</sup> Depto. Volcanología, Instituto de Geofísica, UNAM. Cd. Universitaria, Mexico, D.F., Mexico. E-mail: jmec@unam.mx

<sup>3</sup> Depto. Sismología, Centro de Investigación Científica y Educación Superior de Ensenada, (CICESE), Cta. Ensenada-Tijuana 3918, 22860 Ensenada, BC, Mexico. E-mail: fnava@cicese.mx

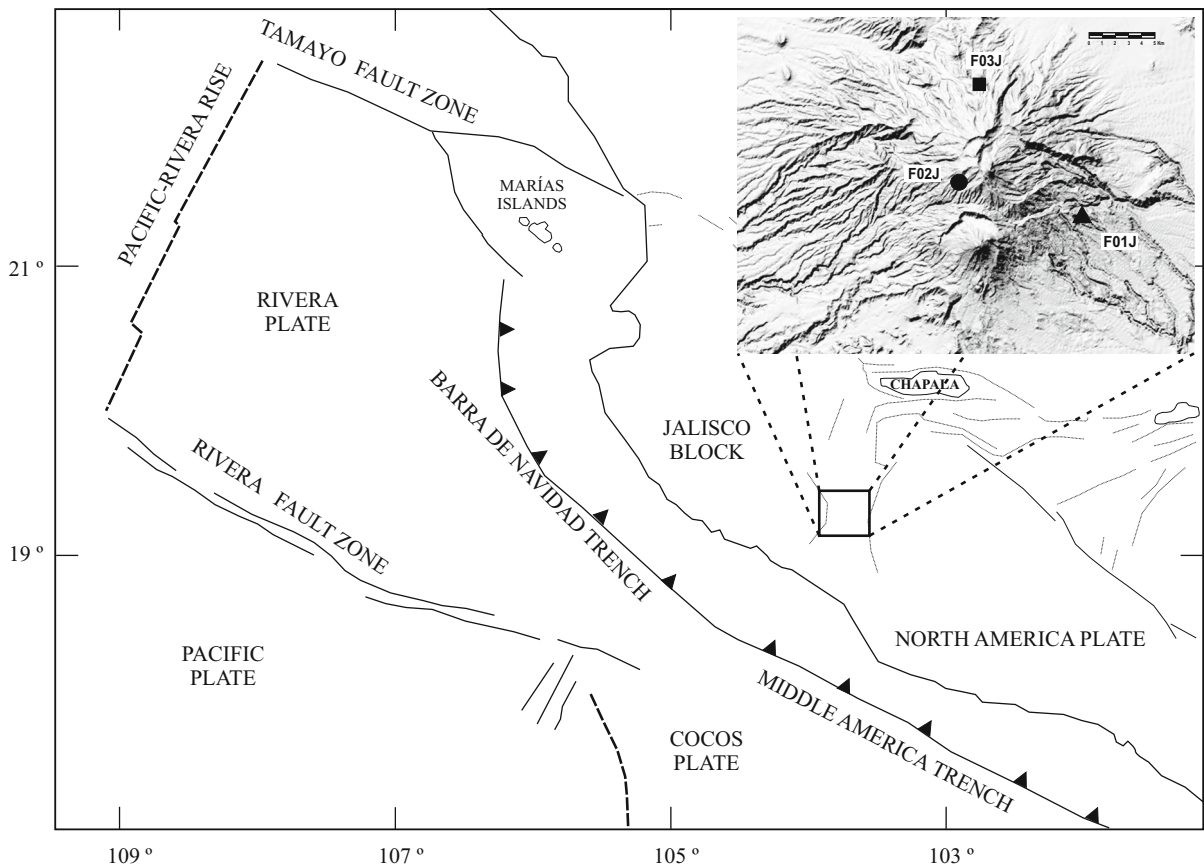


Figure 1  
Tectonic setting of Jalisco block region and location of Colima Volcano

as well to the condition of the volcanic system; that is, in terms of its being closed, partially open, or open. Volcanic earthquakes have been recognized to arise from processes related to faulting in the rock matrix, to the dynamics of the volcanic fluids during magma pressurization or a combination of both mechanisms. The sudden gas decompression produced when the pressure exceeds the strength of the rock cap generates seismic waves that are followed by those that propagate through the atmosphere (NÚÑEZ-CORNÚ *et al.* 2010).

Due to our lacking sonic or pressure sensor data for our analysis we use only the signal registered at the seismometers. It is clear that the frequency observed for the sonic airwave coupling at the seismic stations is a function of the response of the seismometer and the ground at the site. NÚÑEZ-CORNÚ

*et al.* (2010) observed several frequency peaks for explosions that occurred between 1999 and 2003: in seismic stations located at distances between 6 and 10 km, frequency peaks between 11 and 14 Hz associated with a coupled air shock wave (audible, as reported by observers) called shock airwave (SAW), and frequency peaks between 31 and 33 Hz associated with the pressure (infrasonic) airwave coupled airwave, called pressure airwave (PAW).

The complete seismic signal that we observe, generated by a vulcanian explosion is thus characterized by the following process:

- (a) The injection of magmatic material (fluids, gas, ash, debris, etc.), which later reaches the vent.
- (b) The ejection of magmatic constituents into the atmosphere, which generates a PAW, and

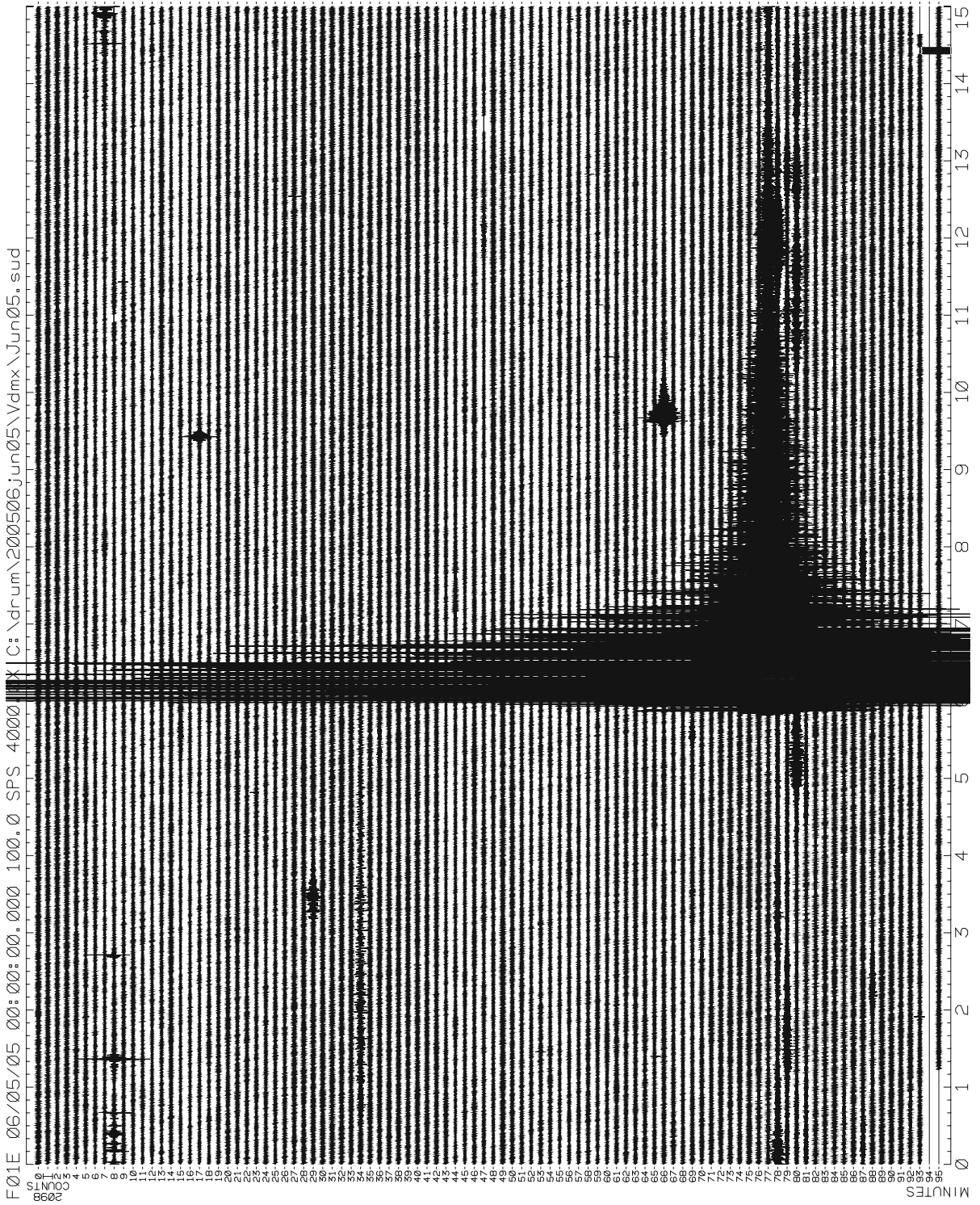


Figure 2  
Sample helicorder seismogram at station F01J (component EW) showing the absence of precursory activity before the explosive event number 12 (May 6, 2005)



possibly a SAW. The ejection process involves coupling between the PAW and SAW (or only PAW) and the ground at the summit.

- (c) The flux of magmatic material through the conduit and the fall of ejecta from the eruptive column.
- (d) The travel path of the seismic signal, and finally
- (e) The ground coupling of the PAW and SAW (or PAW) at the seismic station.
- (f) We illustrate these below, processes through the analysis of the main eruptions of the 2003–2005 cycle.

## 2. Data and Methods of Analysis

The activity of 2003–2005 was recorded by the RESJAL (*Red Sísmica Telemétrica de Jalisco*)

network, operated by *Protección Civil Jalisco* and *SisVOc, Universidad de Guadalajara*. The network consists of three telemetered stations on the volcano: F01J, F02J, F03J (Fig. 3); RESJAL operated four more stations in northern Jalisco. Each station is equipped with a 3-component 1 Hz Lennartz Le3D seismometer (NÚÑEZ-CORNÚ *et al.* 2010) and a 24-bit Everest-Kinematics digitizer recording at 100 samples per second. We studied the 16 larger explosions (Table 1) recorded by RESJAL using data mainly from station F03J located 12 km north of the summit crater. This station was selected because it operated continuously during the study period. Data from the other stations were used to construct record sections for individual explosions to obtain S–P times.

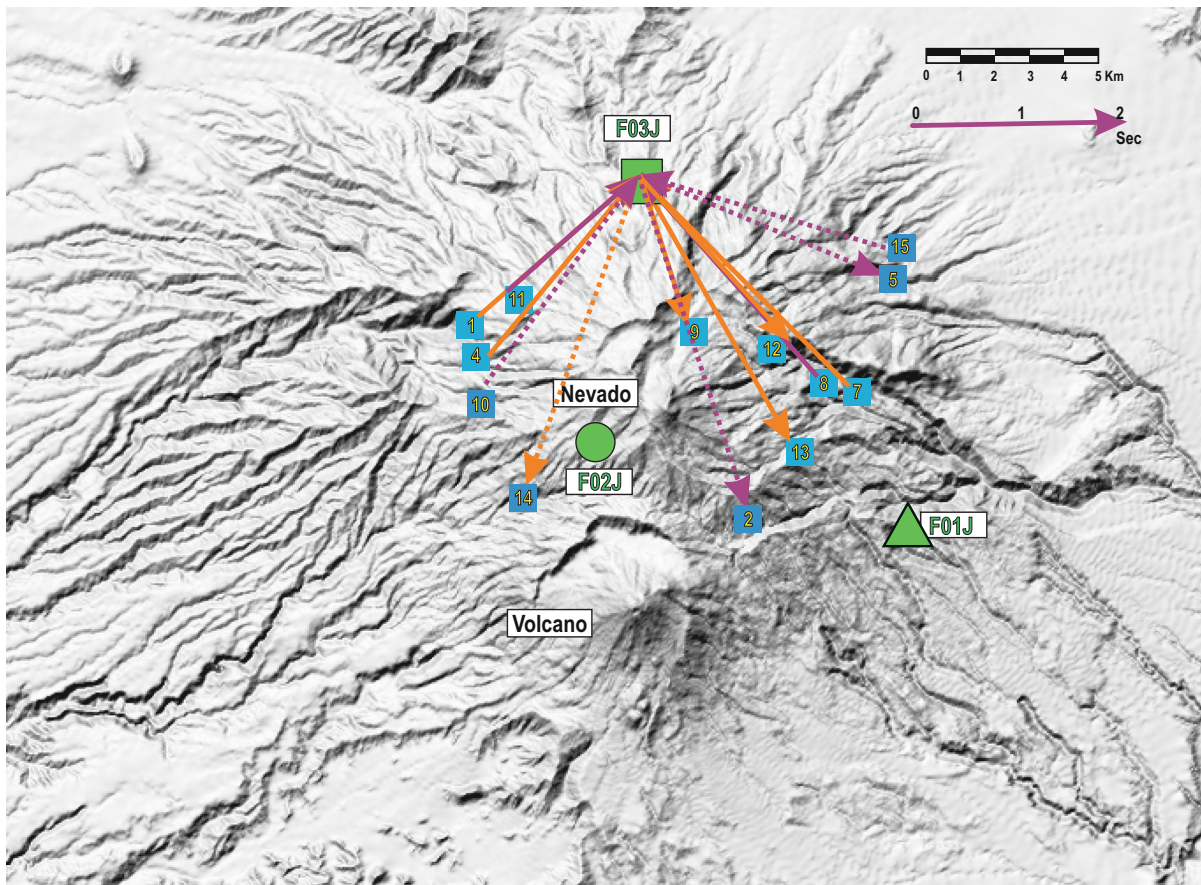


Figure 3

Digital elevation model of the Colima Volcano area displaying seismic station locations. *Solid green triangle* station F01J; *solid green circle* station F02J; *solid green square* station F03J. Numbers refer to explosions listed in Table 1. Arrows show azimuths calculated from first arrivals at F03J; *Orange* P-wave polarized vertically; *Purple* P-wave polarized horizontally; *Dotted arrows* dilatation in the vertical component

Table 1

*Vulcanian explosions at Colima Volcano 2003–2005*

No.	Year	Month	Day	Hour	SoundVel (m/s)	PAW T0 (s)	Vp (km/ s)	P- wave T0 (s)	F03- Pol P-wave	Dif T0 (s)	F03 AzM	F03 S–P	F02 S–P	F01 S–P	F03NS Freq (Hz)	F03NS (PAW) Freq (Hz)
1	2003	July	17	10:27	325	30.03	8.00		V		228	2.04			1.08	31.93
2	2003	August	2	20:41	310	34.08	2.35	33.06	H	1.02	162*	3.32		1.31	1.21	32.13
3	2003	August	29	04:52											0.59	29.88
4	2005	March	13	21:27	300	55.00	4.00	56.58	V	−1.58	200	2.23		2.18	1.21	10.84
5	2005	March	26	03:40					H		112*	2.51			1.20	27.73
6	2005	April	20	01:56											0.56	10.84
7	2005	May	10	14:26	334	56.10	5.50	56.48	V	−0.38	135	2.82	2.26		1.21	28.42
8	2005	May	16	02:01	320	34.20	5.20	34.98	H	−0.78	138	2.55	1.65	1.60	0.89	10.94
9	2005	May	24	00:09	328	45.50	5.80	43.22	V	2.28	162	1.51	1.13		0.96	10.94
10	2005	May	30	08:37	338	21.00	8.00		H		216*	2.53	1.76		0.98	10.64
11	2005	June	2	04:59	336	60.15	6.50		H		228	1.66	0.90	3.58	1.20	28.91
12	2005	June	6	19:20	342	45.99	5.00		V		138	2.13	2.15	2.98	1.20	28.12
13	2005	June	10	02:52	338				V		150	2.91	3.00	2.96	0.54	30.76
14	2005	July	27	09:14	328	32.80	8.00		V		200*	3.13		3.66	1.20	31.30
15	2005	September	16	15:45	345	50.00	7.00		H		106*	2.43	1.16	1.51	0.90	11.04
16	2005	September	27	10:06								3.07	2.47	1.9	1.06	11.72

*SoundVel* Sound velocity as obtained from record sections, *Vp* P-wave velocity as obtained from record sections, *PAW* origin time of the pressure airwave as obtained from the record section, *P-wave T0* origin time of the P-wave obtained from the record section, *F03-Pol P-wave* P-wave polarity at station F03, *Dif T0* time difference at source between P-wave and PAW, *F03 AzM* arrival direction from particle motion at F03, *F03 S–P* S–P time at F03, *F02 S–P* S–P time at F02, *F01 S–P* S–P at F01, *F03NS* peak frequency of the complete signal in the NS component, *F03NS (PAW)* is the PAW peak frequency in the NS component

\* dilatation on vertical component

The N–S and E–W components at F03J were not rotated, as it is deployed approximately along the radial and transverse directions with respect to the summit crater. We used 120 s samples beginning 10 s before the onset of the P-wave. For each record, we calculated the raw spectrum and spectrogram.

Separation of the different trains that compose the seismograms was achieved by band-passing the N–S component between 0.2–1 and 20–40 Hz with a Butterworth recurrent filter (HAVSKOV and OTTE-MÖLLER 1990). For events recorded at more than one station, we constructed record sections to estimate propagation velocities, as well as origin times from the various sources, seismic and explosive (acoustic).

The onset times of the different seismic phases were determined manually from screen-enhanced images of the filtered signals (picking precision  $\leq 0.04$  s).

### 3. Results

Figure 4 shows the raw spectrogram, the spectrum, and a section of the spectral frequency window

between 10 and 40 Hz, for the 16 explosions analyzed. The energy from the SAW and PAW components (NÚÑEZ-CORNÚ *et al.* 2010) can be clearly seen. It is also clear that each event exhibits different patterns. The seismic signals have dominant frequencies in two bands, one centered at about 1.20 Hz and the second below 1.00 Hz. The frequency of the coupled SAW ranges between 10 and 14 Hz, and that of the coupled PAW between 28 and 33 Hz. In six cases the frequency peaks are at 10–14 and 28–33 Hz (events 1, 2, 5, 7, 12, and 13), corresponding to the SAW and PAW phases which are clearly distinguished (NÚÑEZ-CORNÚ *et al.* 2010). In the events 4, 6, 8, 10 and 16 they are barely seen.

Figure 5 shows raw and band-passed seismograms from the N–S component of F03J. The seismograms were filtered between [0.2, 1.0] and [20, 40] Hz. Filtering allows identification of common elements in the events. No conspicuous similarities are observed in the raw waveforms, except for the SAW phase; which is clearly discernible for the 10 May 2005 and 10 June 2005 events. The low-pass

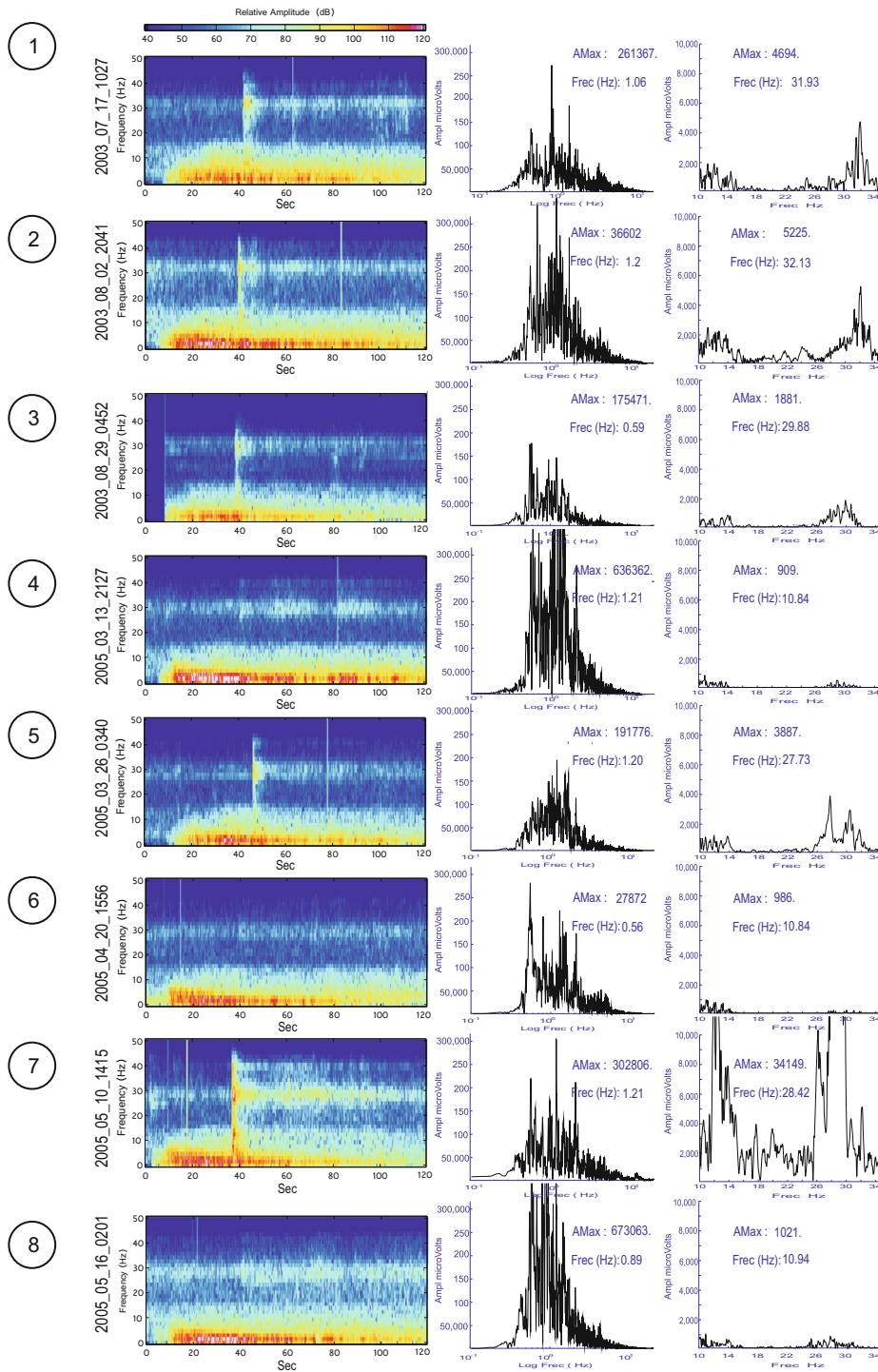


Figure 4

Raw spectrogram, spectrum and close-up of the spectrum for the 16 vulcanian explosions (window between 10 and 40 Hz). Numbers in the left column are dates in yyyy\_mm\_dd\_hhmm format; numbers above spectra are maximum amplitude and peak frequency



Vulcanian Explosions at Colima Volcano

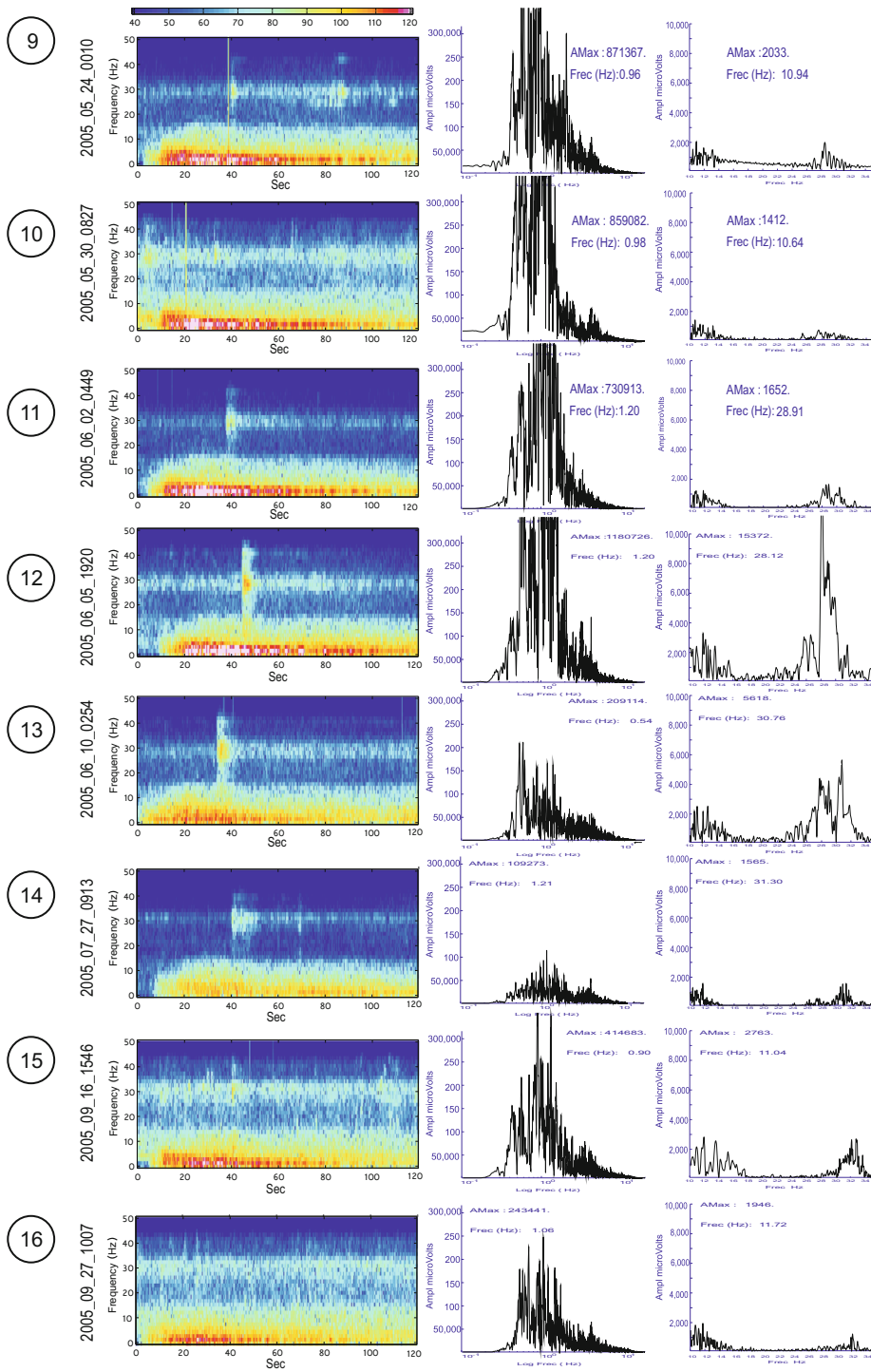


Figure 4 continued

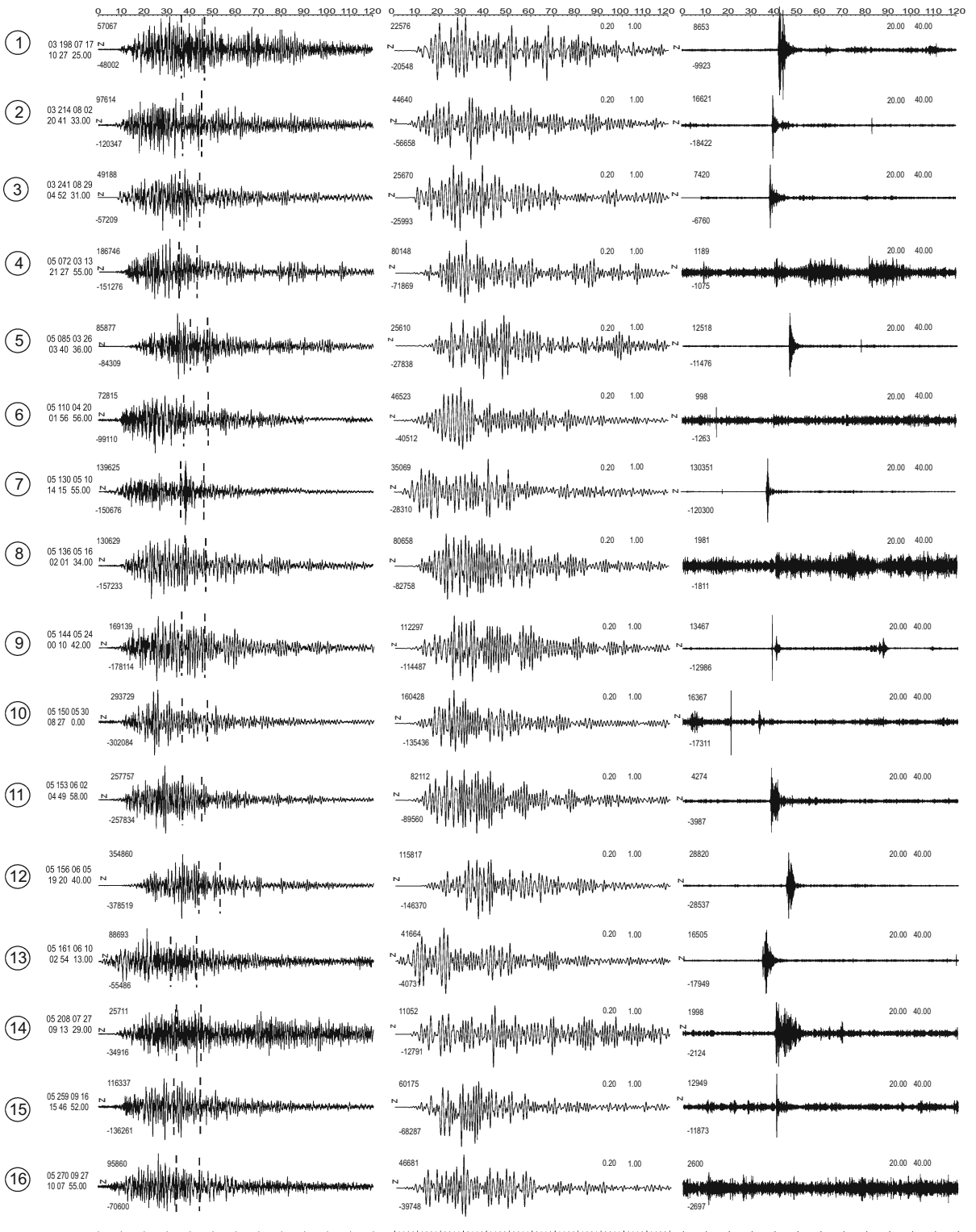




Figure 5

N-S component seismograms recorded at F03J for the 16 explosions, raw and band-pass filtered [0.2, 1.0] and [20.0, 40.0] Hz. Numbers in the *left column* are dates in yyyy\_mm\_dd\_hhmm format; *dashed lines* indicate estimated PAW arrival interval on non filter seismogram; *above* and *below* each seismogram are the maximum and minimum amplitudes in microvolts, below the maximum amplitudes are shown the band-pass filter limits

filtered signals show multiple episodes of energy release. The high-passed waveforms clearly display the PAW in events 1, 2, 3, 5, 7, 11, 12, 13, and 14; while it is absent (or below noise level) for events 4, 6, 8, and 16. It is probably present in the remaining events, albeit with small amplitude.

We made record sections of the coupled airwaves (PAW and/or SAW) recorded at our seismic stations, assuming the crater summit as the location of the

source (Fig. 6). With this procedure, we were able to estimate the velocity of sound, using the reduction velocity around the volcano at the time of the explosions, and the explosion origin time (McNUTT 1986; NÚÑEZ-CORNÚ *et al.* 2010). The estimated sonic velocities are displayed in Table 1. While the estimated sound velocities are reasonable considering the atmospheric conditions around the volcano (JOHNSON 2003), the values obtained from the P-wave arrivals are not, except for event 2 (2.35 km/s), which agrees with a reasonable velocity model for the volcano (NÚÑEZ-CORNÚ *et al.* 2010); a result which can be easily explained assuming different locations of the seismic sources as opposed to those of the explosion sources (PAW and SAW) if we assume the explosion take place at the summit crater.

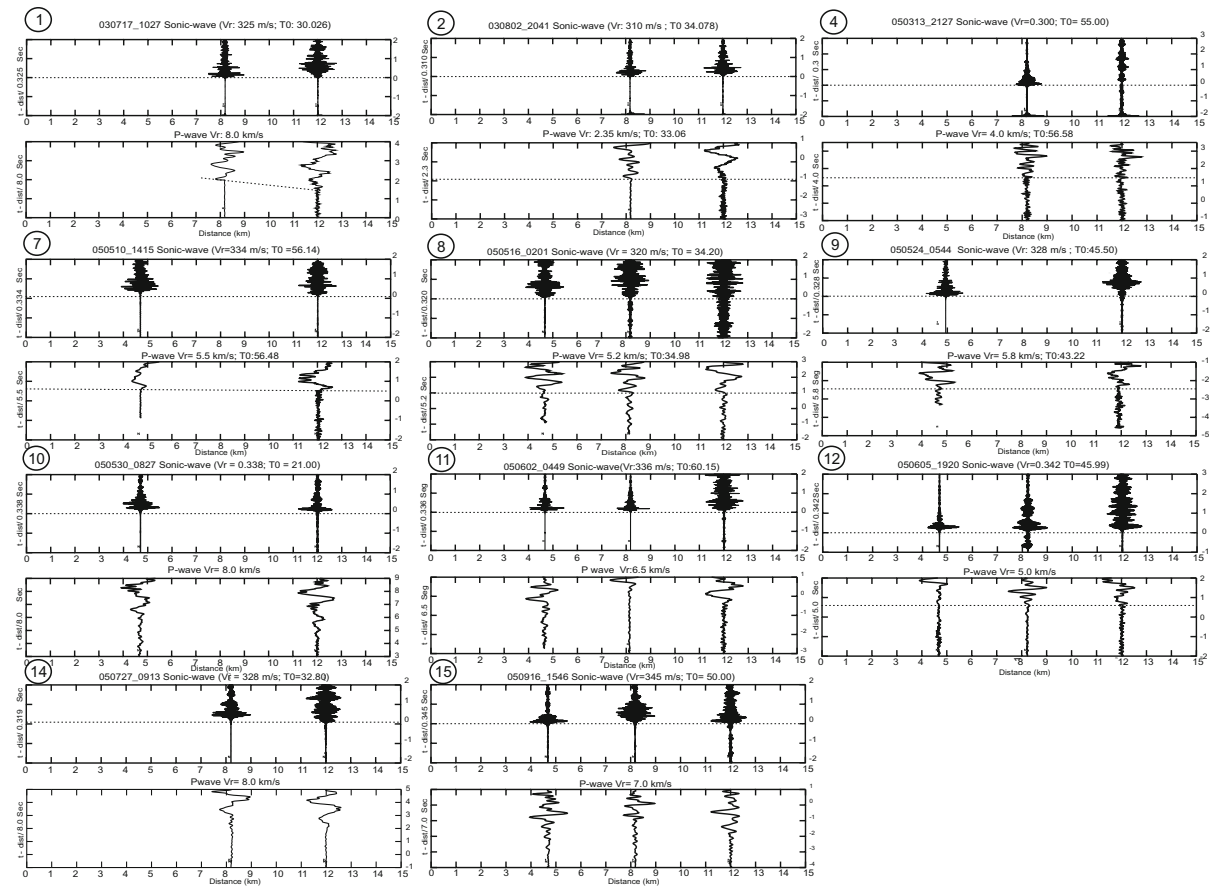


Figure 6

Record sections for P-waves and explosions (PAW) recorded at more than one station

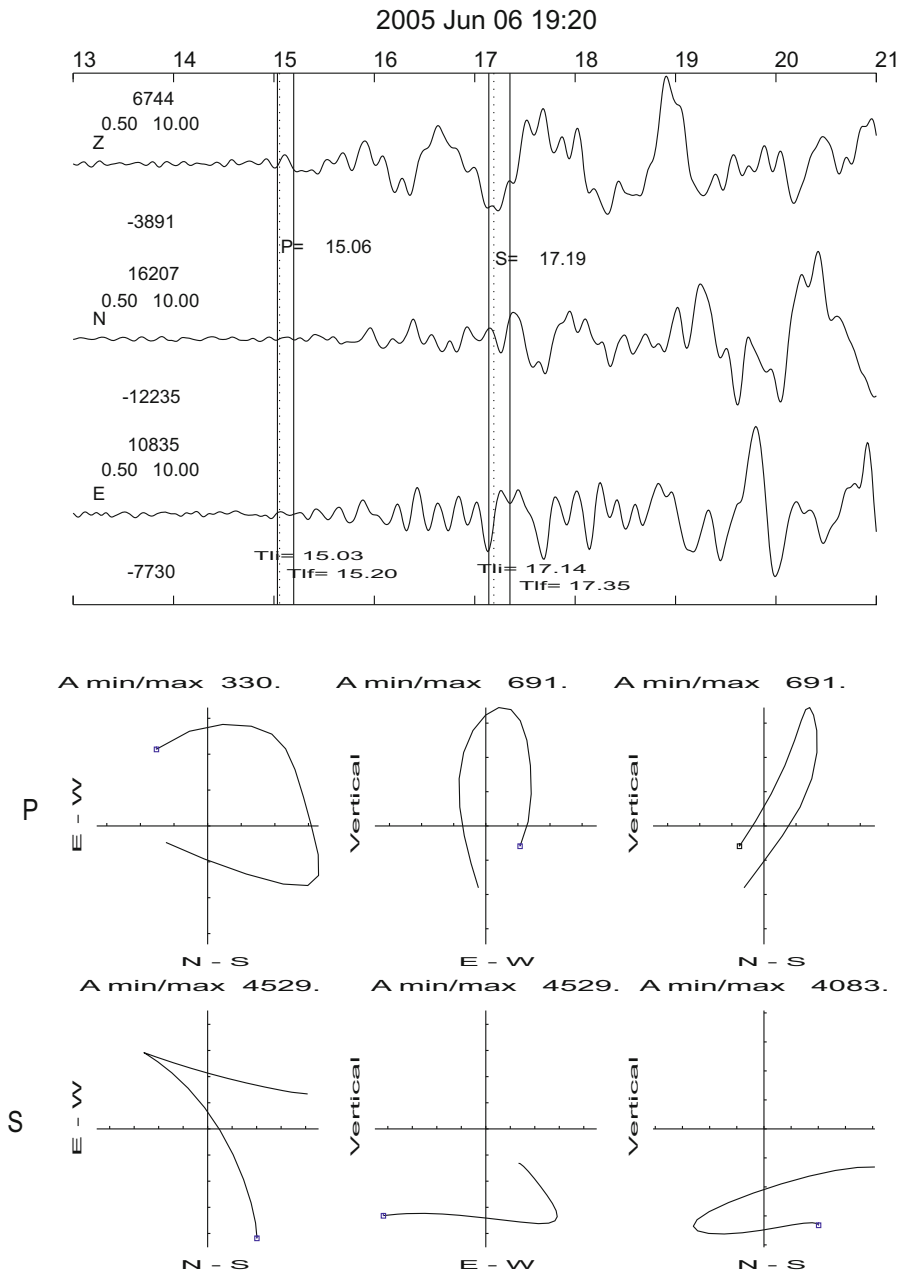


Figure 7  
Example of seismic phase and polarity determination using particle motion

To support this assumption, we identified P and S wave arrivals (Fig. 7) using particle motion to identify polarity within an interval of 0.2 s, and used first motion P-wave amplitude to estimate back azimuths and the approximate direction of source locations (Table 1). This procedure is sometimes of limited reliability due to the influence on particle motion of

diverse conditions such as topography, and internal structure of the medium (MÉTAXIAN *et al.* 2009); however, in our case it yielded consistent results. F03J S–P times range from 1.51 to 3.32 s (Table 1) implies a range distance to the source, epicentral and depth combined, of 6.83 to 15.01 km, assuming a  $V_p = 3.3$  km/s (NÚÑEZ-CORNÚ *et al.* 2010). In the

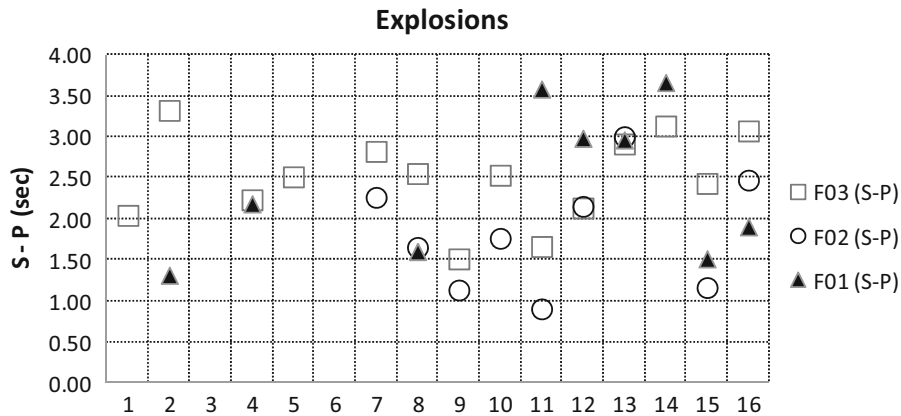


Figure 8  
Distribution of S-P times recorded for each explosions at the stations used in this study

case of F02J the range distance, epicentral and depth combined, to the source is 4.07–13.56 km. We note that the different polarities of the P-wave arrivals (on the three components) and the polarization of the P-wave particle motions agrees with the existence of different fault orientations or sources proposed by HILL (1977). In Fig. 8, we plot the S-P times available for the three stations and each explosion, from which it is possible to conclude that the source of the P-waves is different for each explosion.

#### 4. Discussion and Conclusions

At many volcanoes, it is assumed that P-waves and explosions have a common source. Our results indicate that each vulcanian explosion is preceded by a P-wave generated at a different location from that of the explosion center. These sources operate at different places for the various explosions, as follows from the differences in the P-wave to sonic-wave source time offsets. This observation suggests multiple different fluid pathways discharging to the summit crater area, where the over-pressurized fluids can cause explosions.

Our results support diverse scenarios corresponding to various conditions of fluid pressure: The presence of SAW phases documents conditions of over-pressurized fluid (MORRISEY and MASTIN 2000), while PAW generation accompanied by ash and gas emissions, or the simple emission of ash and gas with

no coupled wave signal at the seismic station, indicate low pressure conditions. Such variation in pressure conditions and the ensuing degassing phenomena are observed in the activity of several volcanoes; for example, NISHIMURA *et al.* (2012) found different pressure conditions between gas bursts and vulcanian eruptions occurring in 2007 and 2010 at Semeru Volcano, Indonesia. At Colima, the distinct energy release pulses are revealed in the low-pass filtered seismograms, which indicate that magmatic parcel fluxes are episodic, rather than single events.

The azimuthal distribution of the foci obtained from P-wave first arrivals, S-P times, and the distance of F03J to the hypocentral area reported by NÚÑEZ-CORNÚ and SANCHEZ-MORA (1999) suggest that the P-wave sources have a shallow distribution beneath the volcano. This agrees with a post brittle/ductile seal breakage state described in the FOURNIER (1999) model, in which the hypocenter depth resides at the depth of the transition where the outer, brittle material provides a seal to the pressurized gases evolving from the magma below.

Vulcanian explosions are the ending phase of a series of processes that begin with the forcing of volcanic fluids through the rock matrix; this process involves the opening or propagation of fractures or faulting. Therefore, the magmatic parcels ejected from the crater originate from various shallow sources beneath the edifice, with pathways that merge at the summit.



### Acknowledgments

We are grateful to Charlotte Rowe for her fruitful observations and valuable comments that greatly improved the manuscript. We appreciate the constructive reviews from two anonymous Referees. This research was partially funded by CONACyT-FOMIXJAL projects 2008-04-96567 and 2012-08-189963. The participation of F. Nava was supported by CONACyT project I0007-2010-01-144588.

### REFERENCES

- DÍAZ, S. (1906). Efemérides del Volcán de Colima, Observatorios de Zapotlan y Colima, de 1893 a 1905. Imprenta y Fototipia de la Secretaría de Fomento. MEXICO, 199 pp.
- FOURNIER, R. (1999). *Hydrothermal processes related to movements of fluid from plastic into brittle rock in the magmatic-epithermal environment*. *Econo. Geol.* 94, 1193–1211.
- HAVSKOV, J. and OTTEMÖLLER, L. (1990). *SEISAN earthquake analysis software*. *Seism. Res. Let.* 70, 532–534.
- HILL, D. (1977). *A model for earthquake swarms*. *J. Geophys Res* 82: 1347–1352.
- JOHNSON, J.B. (2003). *Generation and propagation of infrasonic airwaves from volcanic explosions*. *J. Volcanol. Geoth. Res.* 121, 1–14.
- MCNUTT, SR. (1986). *Observations and Analysis of B-Type earthquakes, Explosions, and Volcanic Tremor at Pavlof Volcano, Alaska*. *Bull. Seism. Soc. Am.* 76, 153–175.
- MÉTAXIAN, J.P., O'BRIEN, G.S., BEAN, C.J., VALETTE, B. and MORA, M. (2009). *Locating volcano-seismic signals in the presence of rough topography: wave simulations on Arenal volcano, Costa Rica*. *Geophys. J. Inter.* 179–3, 1547–1557.
- LUHR J and CARMICHEL I (1990). *Petrological monitoring of cyclical eruptive activity at Volcán Colima, México*. *J. Volcanol. Geoth. Res.* 35: 335–348.
- MORRISSEY M and MASTIN L (2000). *Vulcanian eruptions*. In *Encyclopedia of Volcanoes*, H. Sigurdsson (Editor), Academic Press, New York, pp 463–475.
- NISHIMURA T, IGUCHI M, KAWAGUCHI R, SURONO, HENDRASTO M, ROSADI U (2012). *Inflations prior to Vulcanian eruptions and gas bursts detected by tilt observations at Semeru Volcano, Indonesia*. *Bull. Volcanol.* 74, 903–911, doi:[10.1007/s00445-012-0579-z](https://doi.org/10.1007/s00445-012-0579-z).
- NÚÑEZ-CORNÚ, F.J., SANCHEZ-MORA, C. (1999). *Stress Field Estimations for Colima Volcano, Mexico, Base on Seismic Data*. *Bull. Volcanol.* 60, 568–580.
- NÚÑEZ-CORNÚ, F.J., SUÁREZ-PLASCENCIA, C., RUTZ-LÓPEZ, M., VARGAS-BRACAMONTES, D., SÁNCHEZ, J.J., (2010). *Comparison of Seismic Characteristics of Four Cycles of Dome Growth and Destruction at Colima Volcano, Mexico, from 1991 to 2004*. *Bull. Seism. Soc. Am.* 100, 5A, 1904–1927. doi:[10.1785/0120080356](https://doi.org/10.1785/0120080356).
- ROBIN, C., MOUSSAND, P., CAMUS, G., CANTAGREL, J., GOURGAND, A. and VICENT, P. (1987). *Eruptive History of Colima Volcanic Complex (Mexico)*. *J. Volcanol. Geoth. Res.* 50, 99–113.

(Received May 7, 2015, accepted August 13, 2015, Published online August 31, 2015)